Supporting Information

High-Efficiency Blade-Coated Organic Solar Cells Enabled by In-situ Nitrogen-Blowing and Heating Strategy

Yi Jin[1], Rui Hu[1], Di Xie[1], Xiaojie Ren[1], Xiang Huang[1], Yitong Ji[1], Xiaotong Liu[1], Lidong Liang[1], Xueyuan Yang[1], Wenchao Huang[1]*

[1] Key State Laboratory of Advanced Technology for Materials Synthesis and Processing,

School of Materials Science and Engineering, Wuhan University of Technology, 430070, Wuhan, China

Corresponding E-mail: wenchao.huang@whut.edu.cn

Experimental details

Materials: PM6, BTP-eC9, L8-BO and N,N'-bis{3-[3-(Dimethylamino)propylamino] propyl}perylene-3,4,9,10-tetracarboxylate diimide (PDINN) were purchased from Solarmer Materials Inc., Beijing, China. Poly (3,4-ethylene dioxythiophene): Poly (styrene sulfonate) (PEDOT: PSS) aqueous solution (Clevios PVP 4083) was sourced from Heraeus in Hanau, Germany. Other solvents were obtained from Aladdin (Shanghai, China) and Sigma-Aldrich (St. Louis, Michigan, USA) without additional purification.

Device fabrication

All OSCs were manufactured with ITO/PEDOT: PSS/active layer/PDINN/Ag structure. The pre-patterned indium tin oxide (ITO) glass substrate was washed in water, ethanol, and isopropyl alcohol for 15 minutes and then blown with nitrogen. The ITO substrates were covered with a PEDOT: PSS solution with a thickness of approximately 30±10 nm. The PEDOT: PSS film prepared by the spinning-coating method was baked and annealed in 150℃ for 15 minutes, and substrates were transferred to the blade-coating machine. The weight ratio of donors and acceptors is 1:1.2. The active layer films were coated on the substrate with different coating parameters and then annealed in the air for 5 minutes. Then, PDINN was dissolved in methanol (0.8 mg/mL) and spun for 40s at 3000 rpm. Finally, Ag (110 nm) was thermally evaporated at a vacuum pressure of approximately 1×10^{-4}Pa to form an electrode.

For large-area organic solar modules, the film of 5×5 cm ITO was pre-patterned into multiple 7 mm-wide rectangles. After the deposition of PEDOT:PSS/active layer/PDINN, the functional layers were cut with nanosecond laser into subsequent sub-cells. Finally, 100 nm Ag was thermally-evaporated through a shadow mask, establishing an interconnection between adjacent cells at the ITO-Ag interface.

Characterizations

An ultraviolet spectrometer (UV-1900i, Shimadzu, Japan) is used to measure the absorption and transmission spectra. The device's *J-V* curve was measured with metal mask with an area of 0.0675 cm^2 for small-area devices and 12 cm^2 for large-area solar modules. Measurements were made using a voltage sweep range of -0.2 V to 1.0 V. The light intensity was calibrated using standard silicon reference cells certified by the National Renewable Energy Laboratory (NREL, USA). EQE was measured using the solar cell spectral response measurement system (Enli Technology Co., Ltd., QE-R). The light intensity of the system was calibrated with a reference silicon probe (RC-S103011-E) obtained from Enli Technology Co., Ltd. TPC and TPV were measured using a transient photocurrent and photovoltage measurement system (LST-TPC, Shanghai Jinzhu Technology Co., Ltd.). The morphology of the films was characterized by atomic force microscopy (AFM, Bruker BRUKER Dimension lcon). Grazing-incidence wide-angle X-ray scattering (GIWAXS) patterns were measured using the Xeuss3.0 system. The 10 KeV X-ray beam was incident at a grazing Angle of 0.18°

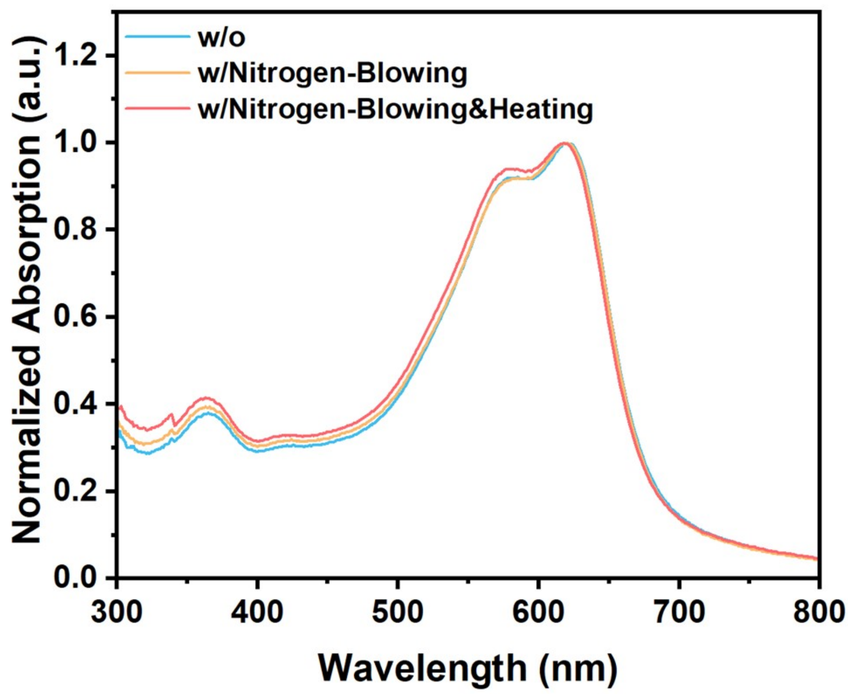

Fig. S1 Normalized UV-Vis absorption spectra of PM6 with different blade-coating methods.

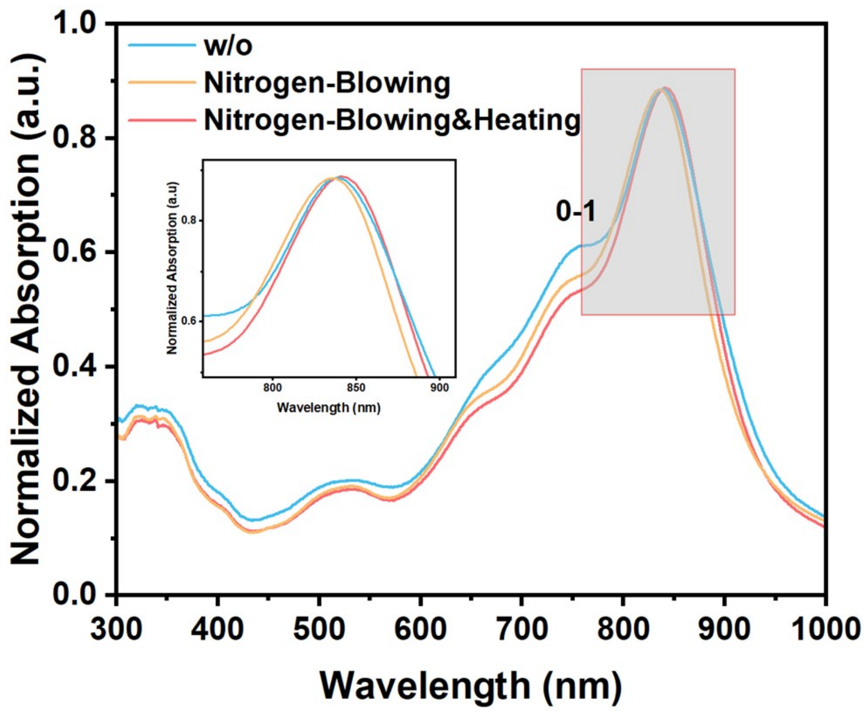

Fig. S2 Normalized UV-vis absorption spectra of BTP-eC9 with different blade-coating methods.

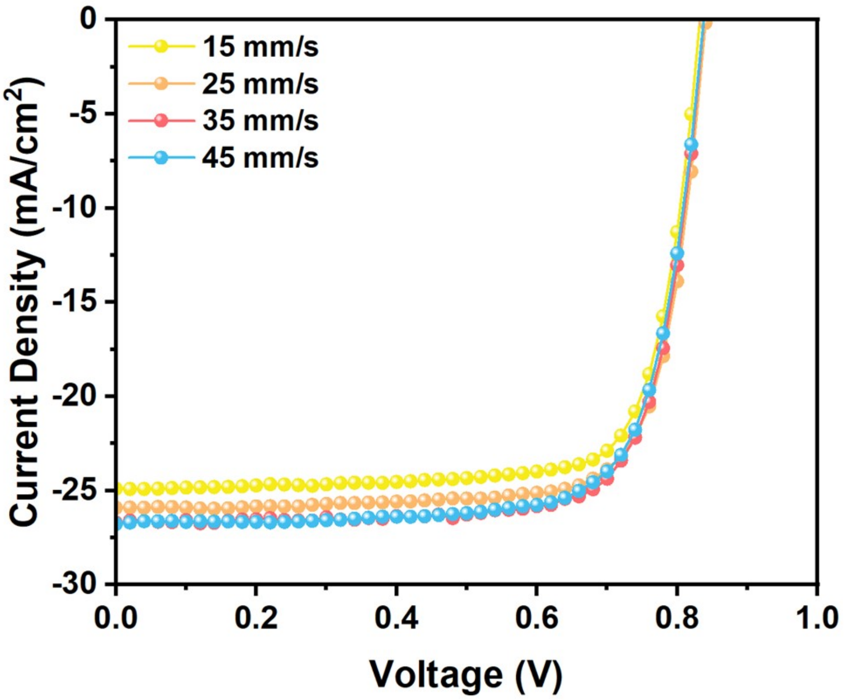

Fig. S3 Device performance of PM6:BTP-eC9-based OSCs devices prepared with blade-coating as a function of blade speed.

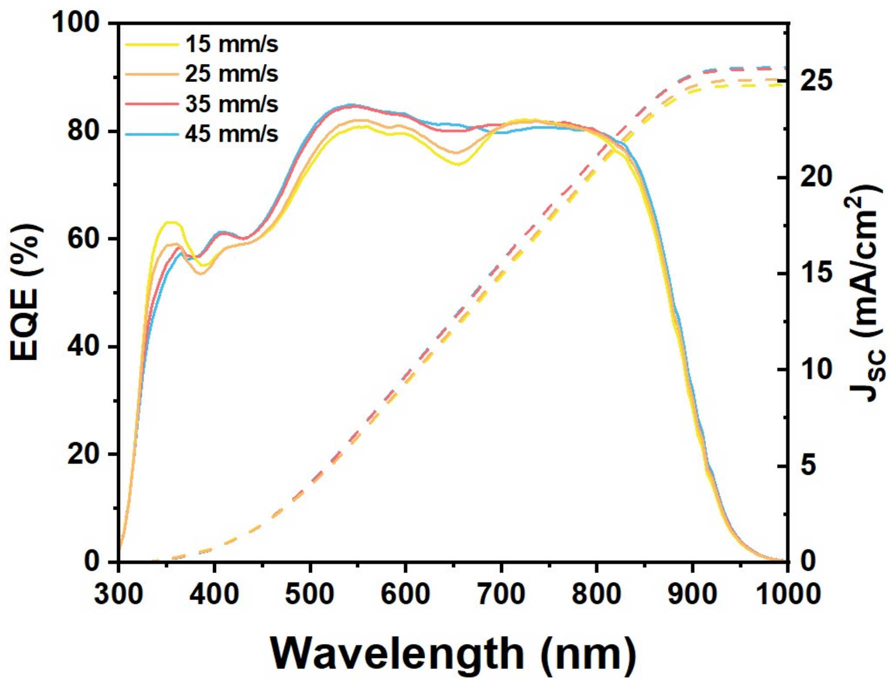

Fig. S4 EQE spectra of PM6:BTP-eC9-based OSCs devices prepared with blade-coating as a function of blade speed.

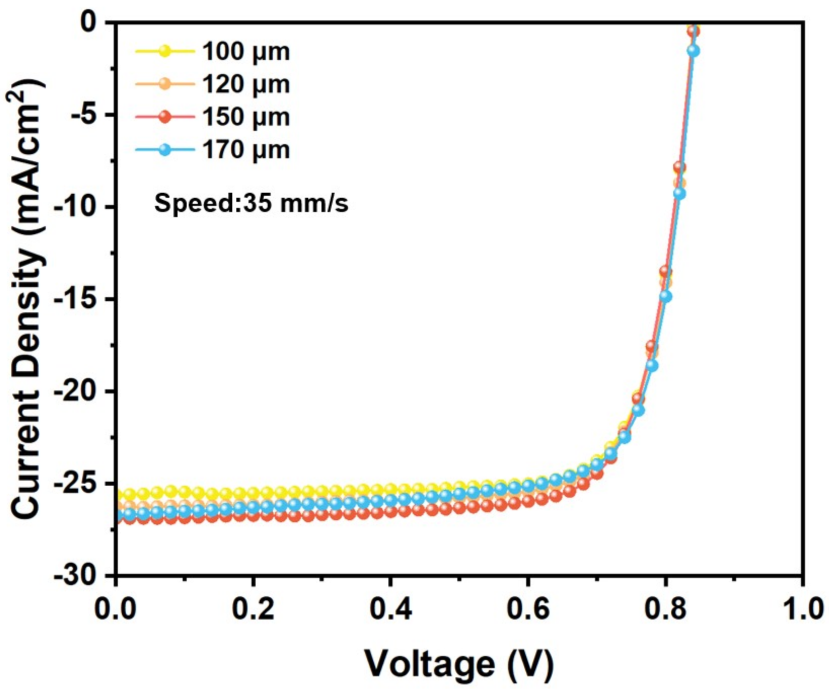

Fig. S5 Device performance of PM6:BTP-eC9-based OSCs devices prepared with blade-coating as a function of blade height.

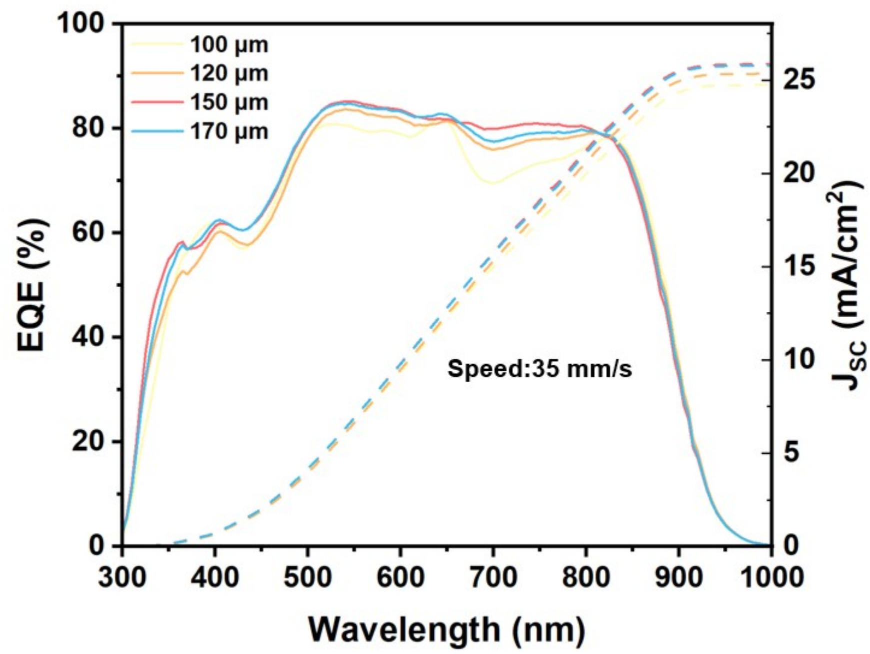

Fig. S6 EQE spectra of PM6:BTP-eC9-based OSCs devices prepared with blade coating as a function of blade height.

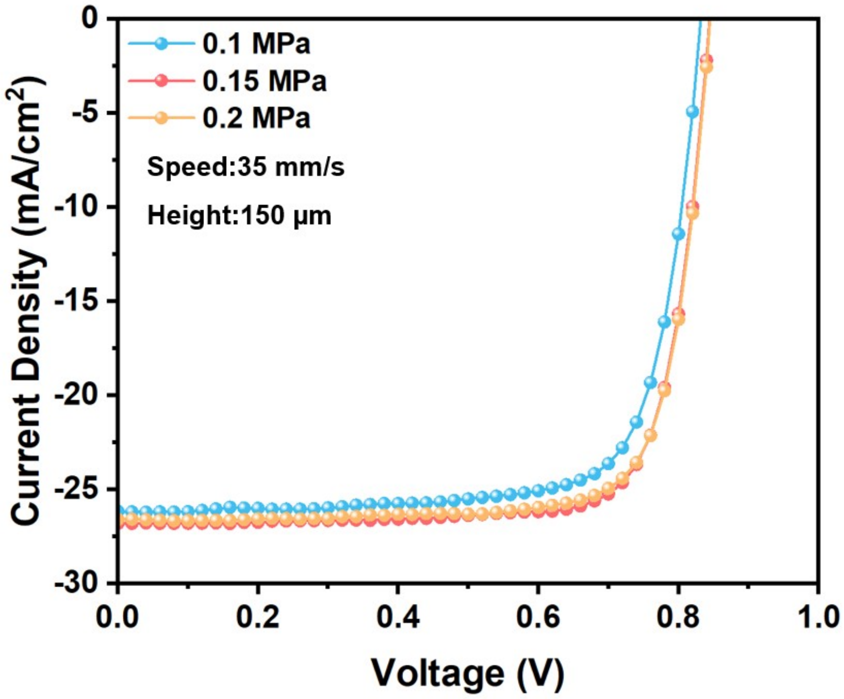

Fig. S7 Device performance of PM6: BTP-eC9-based OSCs prepared with nitrogen-blowing assisted blade-coating method as a function of nitrogen pressures.

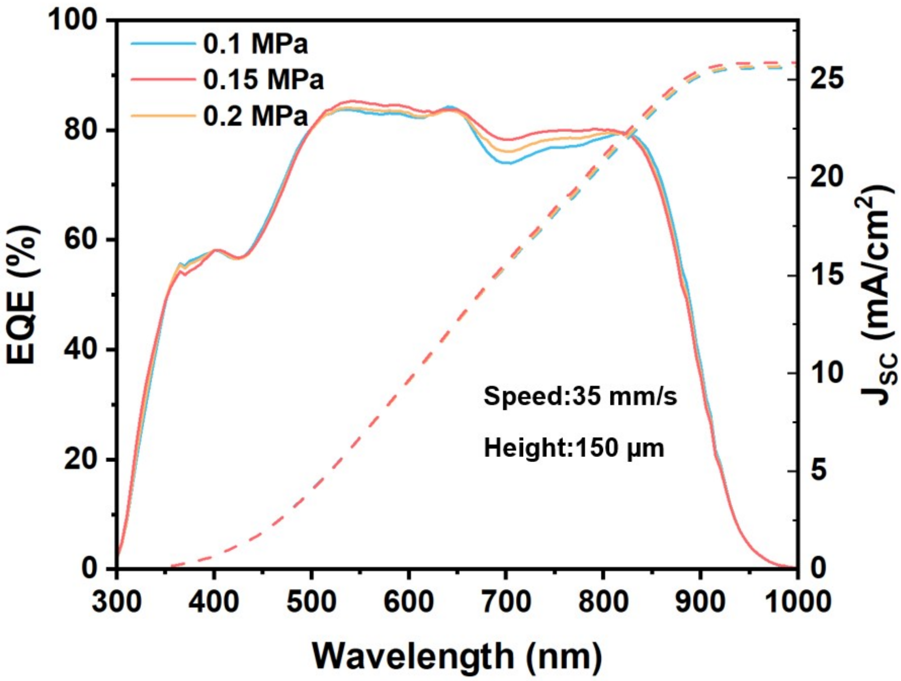

Fig. S8 EQE spectra of PM6:BTP-eC9-based OSCs prepared with nitrogen-blowing assisted blade-coating method as a function of nitrogen pressures.

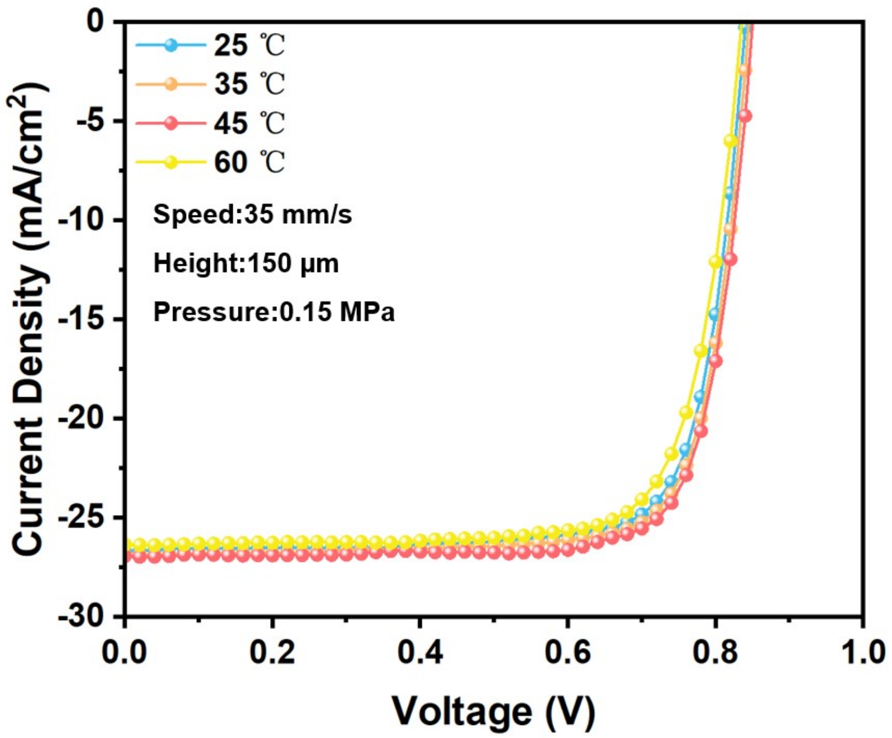

Fig. S9 Device performance of PM6:BTP-eC9-based OSCs prepared with nitrogen-blowing assisted blade-coating method as a function of substrate temperature.

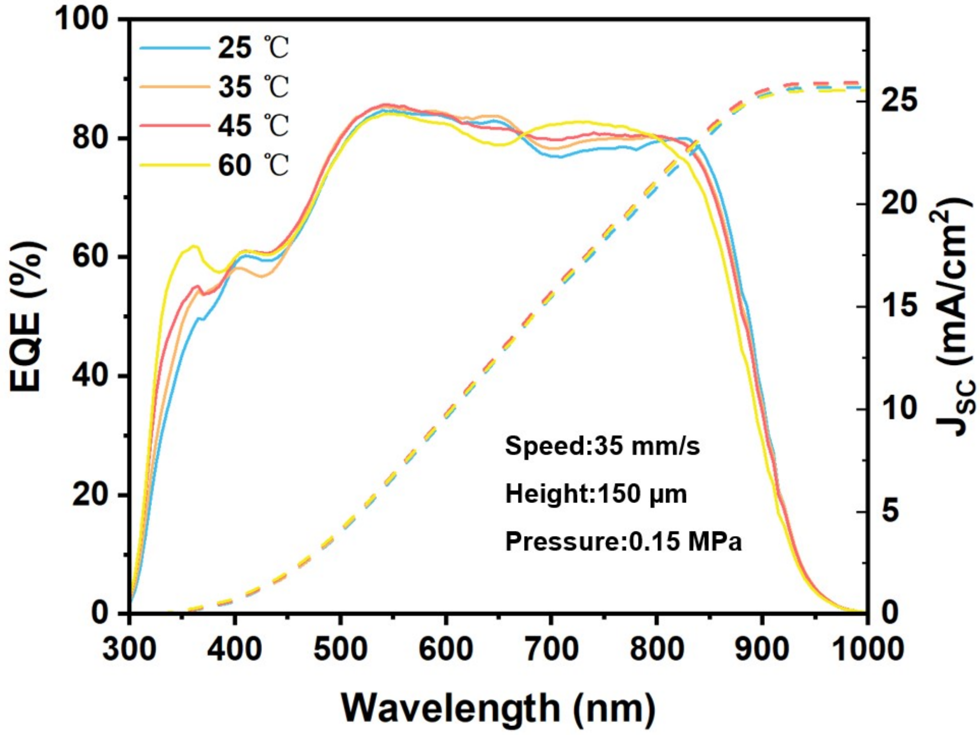

Fig. S10 EQE spectra of PM6: BTP-eC9-based OSCs prepared with nitrogen-blowing assisted blade-coating method as a function of substrate temperature.

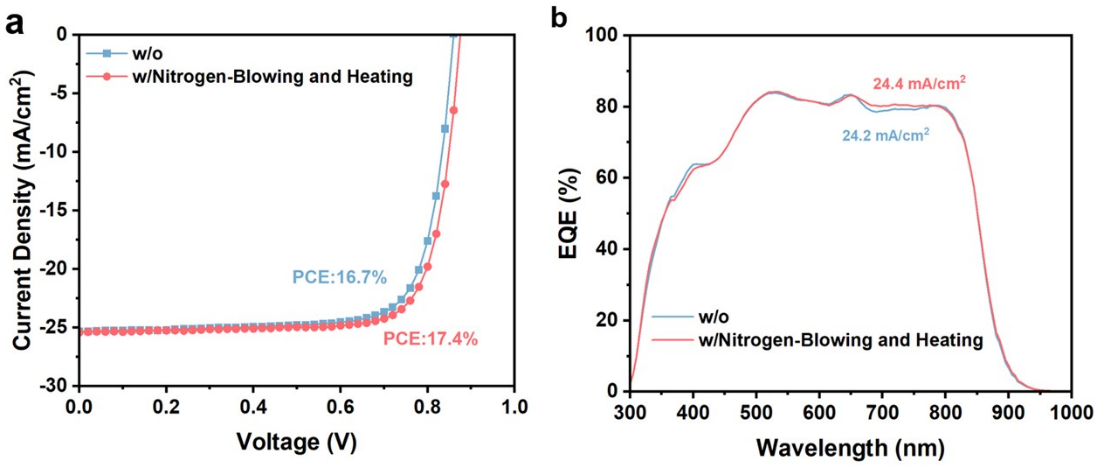

Fig. S11. (a) *J-V* curves and (b) EQE spectra of PM6:L8-BO binary active layer with different blade-coating methods.

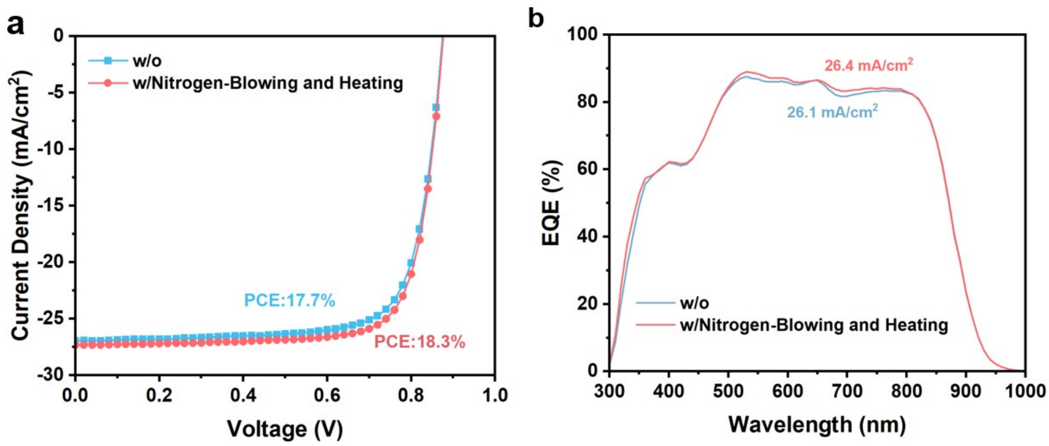

Fig. S12. (a) *J-V* curves and (b) EQE spectra of PM6:L8-BO:BTP-eC9 binary active layer with different blade-coating methods.

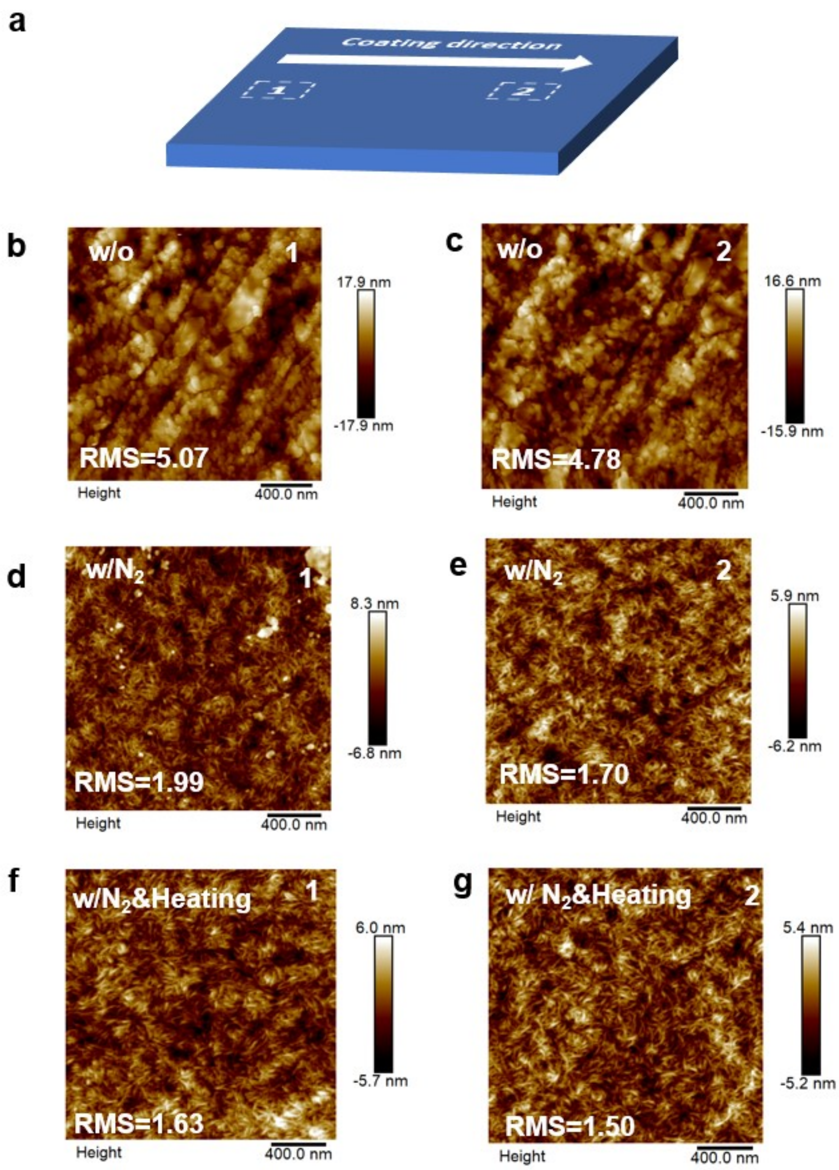

Fig. S13. (a) Diagram of blade-coating. AFM images of the (b) starting and (c) ending position of large-area active layer films based on conventional blade-coating. AFM images of the (d) starting and (e) ending position of large-area active layer films based on nitrogen-blowing assisted blade-coating. AFM images of the (f) starting and (g) ending position of large-area active layer films based on nitrogen blowing and heating assisted blade-coating.

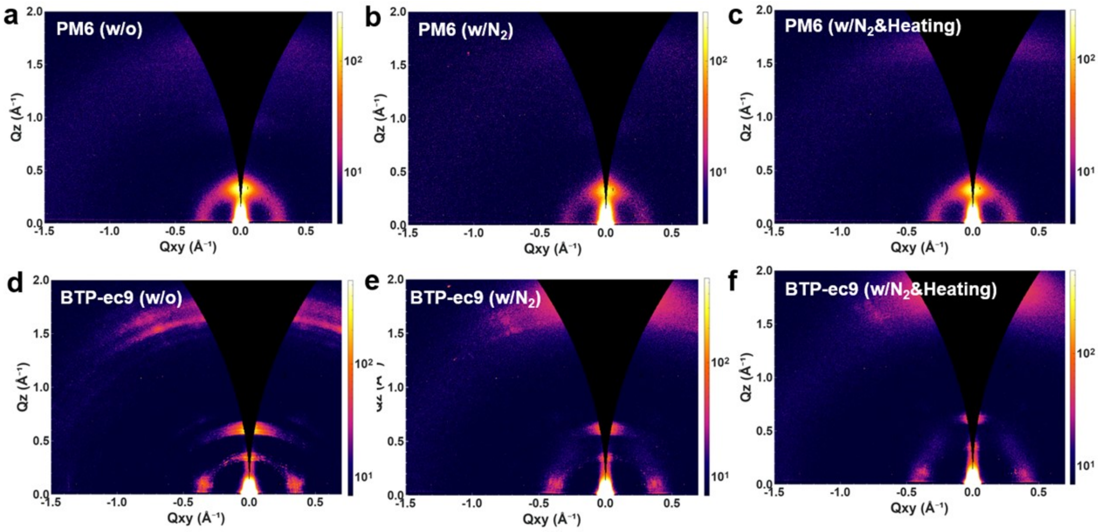

Fig. S14. 2D GIWAXS patterns of the (a-c) PM6 and (d-f) BTP-eC9 films fabricated using different blade-coating methods.

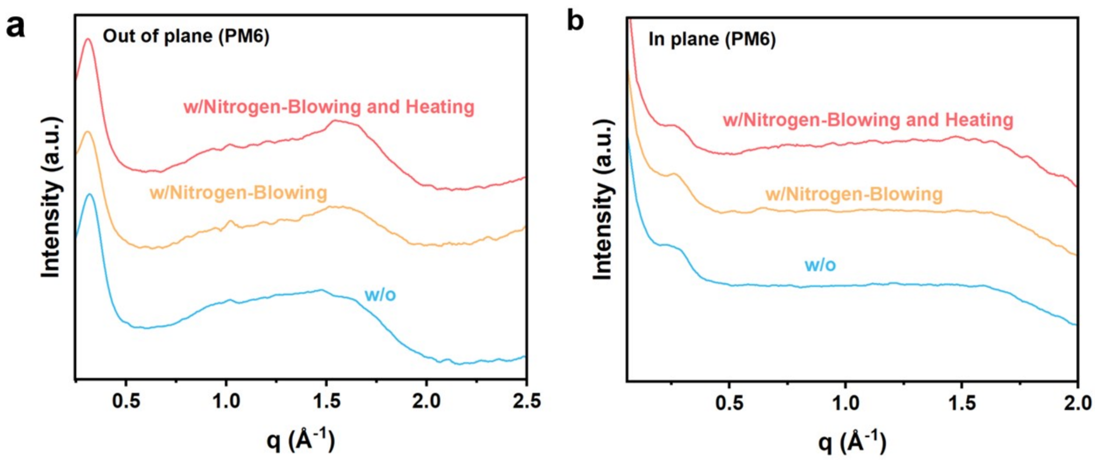

Fig. S15. Integrated scattering profiles for PM6 fabricated using different blade-coating methods along (a) OOP and (b) IP directions.

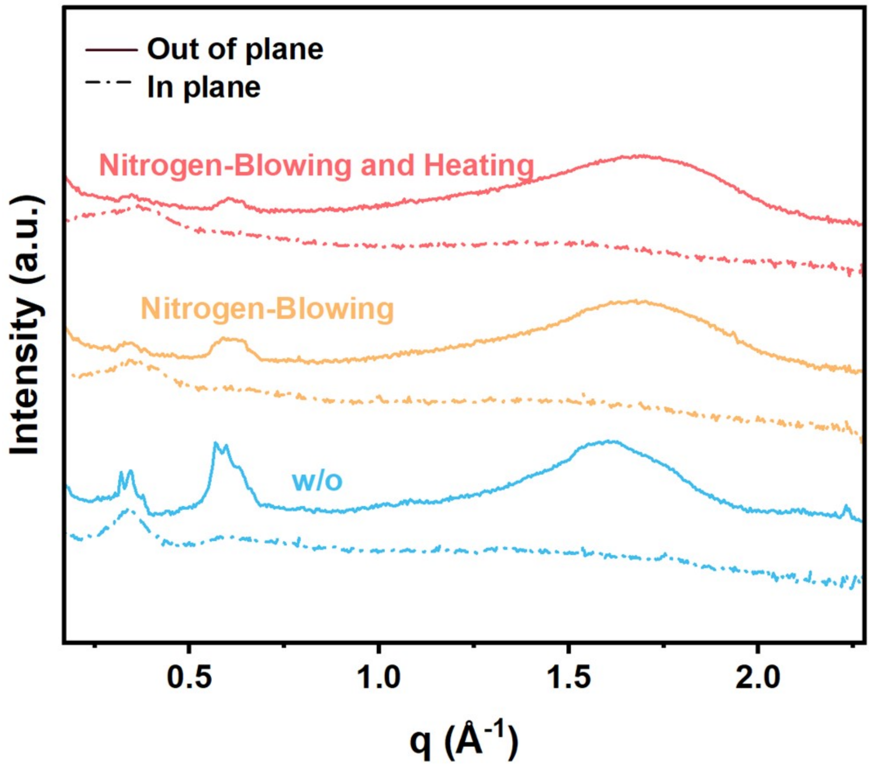

Fig. S16. Integrated scattering profiles for BTP-eC9 films fabricated using different blade-coating methods along OOP and IP directions.

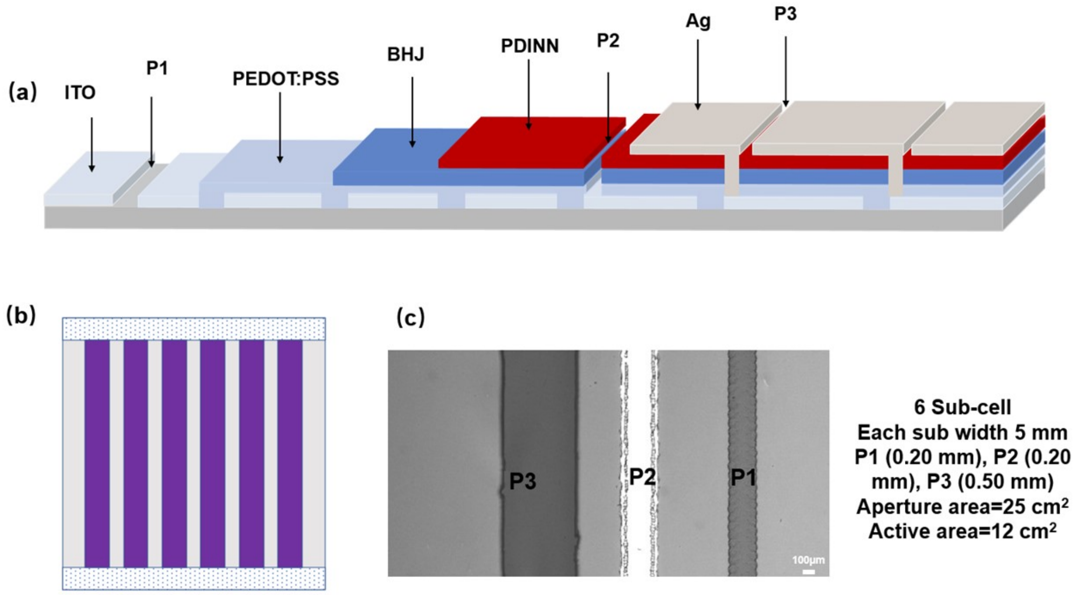

Fig. S17 (a) Schematic diagram of the structure of large-area organic solar cell modules. (b) Schematic diagram of the series structure of 6 sub-cells. (c) Optical microscope images of cutting P1, P2, and P3.

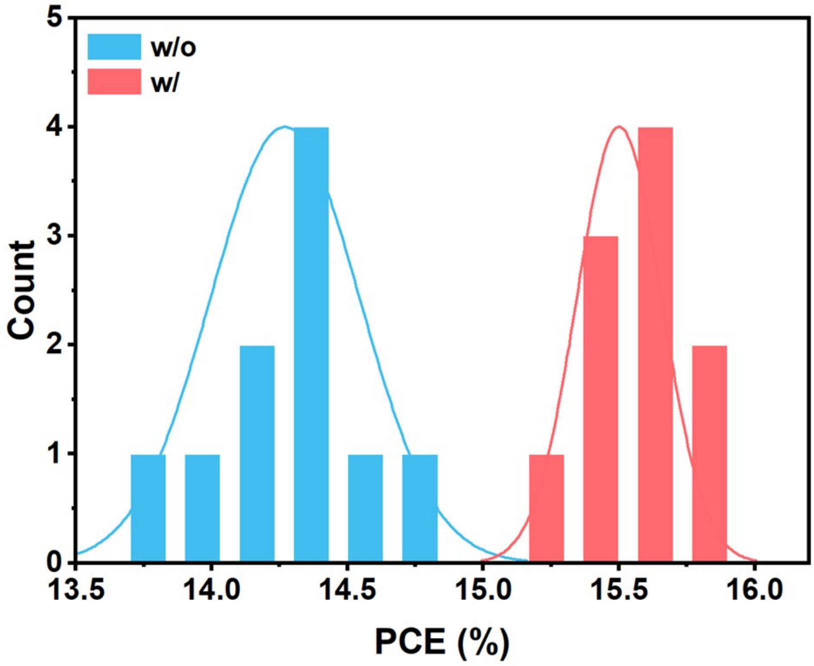

Fig. S18 Efficiency histograms of large-area modules prepared by blade-coating with and without the nitrogen-blowing and heating strategy.

Table S1. Photovoltaic parameters of OSCs prepared as a function of blade coating speed.

Speed (mm/s)	V_{OC} (V)	J_{SC} (mA/cm^2)	J_{EQE} (mA/cm^2)	FF (%)	PCE (%)
15	0.835	24.90	24.8	77.3	16.1
25	0.845	25.9	25.1	76.7	16.7
35	0.843	26.7	25.6	76.1	17.1
45	0.833	26.8	25.8	74.9	16.8

Table S2. Photovoltaic parameters of OSCs prepared as a function of blade heights. (Speed:35 mm/s)

Height (μm)	V_{OC} (V)	J_{SC} (mA/cm^2)	J_{EQE} (mA/cm^2)	FF (%)	PCE (%)
100	0.841	25.6	24.7	77.2	16.6
120	0.845	26.2	25.5	76.2	16.9
150	0.843	26.8	25.8	75.8	17.1
170	0.844	26.5	25.8	74.8	16.7

Table S3. Photovoltaic parameters of OSCs prepared with nitrogen-blowing assisted strategy as a function of nitrogen pressures. (Speed:35 mm/s; Height:150 μm)

Pressure (MPa)	V_{OC} (V)	J_{SC} (mA/cm^2)	J_{EQE} (mA/cm^2)	FF (%)	PCE (%)
0.1	0.835	26.1	25.6	76.0	16.5
0.15	0.843	26.8	25.9	78.4	17.7
0.2	0.845	26.6	25.7	78.2	17.5

Table S4. Photovoltaic parameters of OSCs prepared by blade-coating with nitrogen-blowing and heating assisted strategy as a function of substrate temperature. (Speed:35 mm/s; Height:150 μm; Pressurre:0.15 MPa)

Temperature (℃)	V_{OC} (V)	J_{SC} (mA/cm^2)	J_{EQE} (mA/cm^2)	FF (%)	PCE (%)
25	0.845	26.6	25.7	77.6	17.4
35	0.843	26.8	25.8	78.2	17.7
45	0.852	26.9	25.9	78.9	18.1
60	0.835	26.3	25.54	76.7	16.8

Table S5. The photovoltaic performance parameters of PM6:L8-BO devices by blade-coating without and with nitrogen-blowing and heating assisted strategy

Blends	Treatment	V_{OC} (V)	J_{SC} (mA/cm^2)	FF (%)	PCE (%)
PM6:L8-BO	w/o	0.859	25.3	76.9	16.7
	w/	0.875	25.4	78.0	17.4

Table S6. The photovoltaic performance parameters of PM6:L8-BO:BTP-eC9 devices by blade-coating without and with nitrogen-blowing and heating assisted strategy

Blends	Treatment	V_{OC} (V)	J_{SC} (mA/cm^2)	FF (%)	PCE (%)
Ternary	w/o	0.874	26.8	75.9	17.7
	w/	0.876	27.1	77.3	18.3

Table S7. Information of GIWAXS results for relevant films.

	Samples	q ($Å^{-1}$)	d-spacing (Å)	FWHM ($Å^{-1}$)	CCL (Å)
OOP	w/o	1.69	3.71	0.42	13.43
	w/N_2	1.65	3.81	0.39	14.43
	w/N_2&heating	1.67	3.76	0.38	14.68
IP	w/o	0.29	21.66	0.12	47.12
	w/N_2	0.28	22.44	0.13	41.58
	w/N_2&heating	0.28	22.54	0.13	43.16